

UV Spectra and Excitation Delocalisation in DNA: Influence of the Spectral Width

Emanuela Emanuele^[1], Dimitra Markovitsi^{[1]*}, Philippe Millié^[1] and Krystyna Zakrzewska²

KEYWORDS:

DNA photodamage · UV absorption · excitons · electronic coupling · double helix dynamics ·

¹ *E. Emanuele, Dr. D. Markovitsi, Dr. P. Millié*
Laboratoire Francis Perrin, CEA/DSM/DRECAM/SPAM - CNRS URA 2453
CEA Saclay, 91191 Gif-sur-Yvette, France
fax: (+33) 1 69 08 87 07
E-mail: dimitra.markovitsi@cea.fr

* To whom correspondence should be addressed.

² *Dr. K. Zakrzewska*
Laboratoire de Biochimie Théorique, CNRS UPR 9080, Institut de Biologie Physico-Chimique, 13, rue Pierre et Marie Curie, 75005 Paris, France

ABSTRACT

The present communication deals with the singlet excited states of the model DNA duplex (dA)₁₀.(dT)₁₀. Calculations are performed in the frame of the exciton theory. Molecular dynamics calculations provide the duplex geometry. The dipolar coupling is determined using atomic transition charges. The monomer transition energies are simulated by Gaussian functions resembling the absorption bands of nucleosides in aqueous solutions. Most of the excited states are found to be delocalized over at least two bases and result from mixing of different monomer states. Their properties are only weakly affected by conformational changes of the double helix. On average, the highest oscillator strength is carried by the upper eigenstates. The duplex absorption spectra are shifted a few nanometers to higher energies with respect to the spectra of non-interacting monomers. The states with larger spatial extent are located close to the maximum of the absorption spectrum.

INTRODUCTION

It is well known that absorption of UV light by DNA induces photochemical reactions which may provoke carcinogenic mutations.^[1-2] The first step of such a series of events leading to alteration of the genetic material is the formation of the so-called Franck-Condon excited states, *e.g.* singlet excited states formed instantaneously upon photon absorption, without any prior relaxation. Their characterization is necessary in order to understand how electronic excitation energy is transformed into chemical energy within the double helix.

The main issue regarding the singlet excited states of the double helix is whether they are localized on single bases or delocalized over a certain number of them. Very rapidly the opinion that photons are absorbed by single bases prevailed and guided subsequent photophysical and photochemical investigations involving DNA. This is due to the observation that the DNA UV spectra closely resemble the sum of the spectra of the constituent bases.^[3] The hypothesis underlying this reasoning is that formation of delocalized excited states should induce large shifts in the absorption spectra. Moreover, a visible splitting of the absorption band around 260 nm was expected.^[4-5] Although the first theoretical studies dealing with DNA excitons appeared about forty years ago,^[4, 6-7] the validity of such statements had not been systematically checked. This contrasts with the sophisticated calculations, combining quantum chemistry and molecular dynamics, which have been developed recently to describe charge transfer in DNA.^[8-10]

In the frame of the exciton theory,^[11-12] the excited states of a multichromophoric system are linear combinations of the excited states of each monomeric chromophore. Their properties are obtained by diagonalization of the Hamiltonian matrix, in which the diagonal and off-diagonal terms

represent the excitation energy of the monomer transitions within the examined system and the electronic coupling, respectively. The delicate point in this type of studies is the way that the various terms are calculated. The improvement of computational techniques occurred during the past decades opened the possibility to determine the exciton matrix elements with much higher precision compared to earlier studies. New methodologies, introducing quantum chemistry methods in the calculation of the diagonal and off-diagonal terms, were applied in the investigation of various systems such as molecular aggregates and photosynthetic antennas (see for example references 13-18). Thus, subtle differences appeared in the properties of various systems and the effect of structural disorder could be evaluated.

Following this progress, it became possible to revisit the DNA excited states, examine the various factors which affect their properties and determine their footprint on the absorption spectra. Within this context, we are interested here in the exciton states of the model duplex (dA)₁₀.(dT)₁₀, composed of one strand of adenines and one strand of thymines. This theoretical study is a continuation of two previous investigations on duplexes consisting of adenine – thymine base pairs ^[19-20] which were performed in parallel with experimental spectroscopic studies.^[21-22]

Our first communication^[19] focused on the electronic transitions of the monomers that have to be taken into account in the construction of the exciton matrix and the precision necessary in the calculation of the dipolar coupling. It was shown that it is important to consider two lowest transitions for adenine, $S_0 \rightarrow S_1$ and $S_0 \rightarrow S_2$, which can be coupled with the $S_0 \rightarrow S_1$ thymine transition. Moreover, it was demonstrated that the point dipole approximation, used in the previous DNA studies and known to predict artificially large exciton shifts, is not valid for the

calculation of the dipolar coupling in double helices. It was concluded that the dipolar coupling, calculated using atomic transition charges, can induce delocalization of the electronic excitation with double helices having an idealized B-DNA geometry. Our second communication^[20] examined how the dynamics of the double helix affects the excitons in the same type of duplexes. It was shown that structural fluctuations reduce the spatial extent of the excited states but excitations still remain delocalized over several bases.

In both of the above mentioned publications the hypothesis was made that changes in the internal structure of the monomeric chromophores do not affect the energy of the monomer electronic transitions. Such changes are responsible for the spectral width (homogeneous and inhomogeneous broadening) of the UV absorption bands corresponding to the electronic transitions of monomeric nucleic acids in aqueous solutions. And, precisely, the relative magnitude of the electronic coupling with respect to that of the spectral width is a commonly accepted criterion for formation of localized or delocalized excited states.^[23] The dipolar coupling between transitions of nearest bases in double helices amounts to a few hundreds of wavenumbers, whereas the spectral width of the monomer transitions is about one order of magnitude larger.^[19] Accordingly, one would expect complete localization of the excited states. However, this effect may be compensated by the existence of more than one monomer electronic transitions with different polarizations which can be coupled.^[24]

The objective of the present work is double. Firstly, it intends to examine how the dispersion of the monomer transition energies, combined to conformational changes, may affect the singlet excited states of (dA)₁₀.(dT)₁₀ related to photon absorption. To this end, the monomer transition

energies are simulated by Gaussian functions resembling to the corresponding experimental absorption bands. The associated spectral width is supposed to correspond to homogeneous broadening since our previous calculations have shown that the inhomogeneous broadening does not exceed a few wavenumbers (Figure 3 in reference 20). Secondly, it aims at establishing a correspondence between the absorption spectrum and the properties of the singlet excited states providing some guidelines for experimental photophysical and photochemical studies. In Section 2, the methodology followed in the calculation is outlined in a simple way. The results are presented and discussed in Section 3. Finally, in Section 4 we summarize our findings and we comment on the possible consequences on the photophysics and photochemistry of DNA double helices.

METHODOLOGY

The duplex excited states were calculated in the framework of the exciton theory.^[11- 12] The detailed formalism is described in reference 19. The main points of the methodology followed in the present study are the following.

1. **Duplex geometry.** The ground state conformations used for the calculation of the Franck-Condon excited states of $(dA)_{10} \cdot (dT)_{10}$ were extracted from molecular dynamics simulations including explicitly solvent and counter-ions. The calculation procedure is described in reference 20. The duplex conformation plays a role in the determination of off-diagonal terms of the exciton matrix because the dipolar coupling between electronic transition moments depends on the angle formed by the corresponding vectors.

2. **Monomer transitions.** The lowest transitions for adenine, $S_0 \rightarrow S_1$ and $S_0 \rightarrow S_2$, which can be coupled with the $S_0 \rightarrow S_1$ thymine transition, were taken into account. The oscillator strength and the energy of the maximum associated with those transitions were derived from the experimental spectra of the nucleosides in aqueous solutions, as explained in reference 19 (Table 1).
3. **Diagonal terms.** The excitation energy of each free monomer transition is given by a Gaussian distribution whose width (fwhm) is 2200, 3600 and 4200 cm^{-1} for the $S_0 \rightarrow S_1$ and $S_0 \rightarrow S_2$ transitions of adenine and the $S_0 \rightarrow S_1$ transition of thymine, respectively (Table 1). In each exciton matrix, a set of monomer transition energies belonging to the above Gaussian functions were considered.
4. **Off-diagonal terms.** The dipolar coupling was calculated using the atomic transition charge distribution model. Atomic charges and polarization of the three transitions were derived from quantum chemistry calculations performed on 9-methyladenine and 1-methylthymine.^[19] The coupling corresponding to all the pairs of different bases forming the duplex was calculated.
5. **Eigenstate properties.** Diagonalization of the exciton matrix corresponding to a given duplex conformation and a given distribution of monomer excitation energies yields the k eigenstates of the system (equation 1) which are linear combinations of the wavefunctions $\langle \Psi_n \rangle$ corresponding to the monomer transitions:

$$|k\rangle = \sum_{n=1}^N C_{k,n} |\Psi_n\rangle . \quad \text{[Equation 1]}$$

Since the considered duplex consists of ten adenines, with two transitions each, and ten thymines, with one transition each, it has thirty eigenstates $\langle k \rangle$, whose energy increases from $\langle 1 \rangle$ to $\langle 30 \rangle$.

Table 1

RESULTS AND DISCUSSION

First, we consider the eigenstates of the duplex obtained for one conformation, extracted from molecular dynamics simulations, and a single distribution of monomer energy values chosen randomly. Figure 1A shows the oscillator strength f associated with each one of the thirty eigenstates. We observe that some eigenstates are characterized by f values close to zero and correspond to forbidden electronic transitions. For one third of them, f is smaller than 0.05, value corresponding to the weakest monomer transition ($S_0 \rightarrow S_1$ of adenine). Eight eigenstates have oscillator strength higher than 0.24, value corresponding to the $S_0 \rightarrow S_1$ transition of thymine and the $S_0 \rightarrow S_2$ transition of adenine (Table 1).

Figure 1

The general trend regarding the difference in the oscillator strength between the monomer and the duplex transitions, discussed above, does not depend on the distribution of the diagonal terms. What varies from one distribution to the other is the precise way that the oscillator strength

is spread over the thirty eigenstates, that is, the eigenstates bearing low or high f values. Thus, if we consider the average oscillator strength per eigenstate obtained for 500 sets of free monomer transition energies (Figure 1B), we remark that none of the f values is zero. However, about 80% of the oscillator strength is concentrated at the upper half of the eigenstates (<16> to <30>). In Figure 1B, the results obtained for four different conformations of double helix are shown. The total oscillator strength associated with the duplex transitions (5.02) is somewhat lower than the sum of the oscillator strength corresponding to non-interacting monomers (5.30).

Figure 2

The degree of delocalization of the exciton states is usually quantified by the participation ratio $PR=1/L_k$ which represents the number of coherently coupled chromophores.^[25- 26] When there are more than one electronic transition per chromophore, L_k is given by equation 2.

$$L_k = \sum_{\text{monomer } m} \left[\sum_{\text{states } i} (C_{k,m}^i)^2 \right]^2 \quad \text{[Equation 2]}$$

The sum within the square brackets represents the contribution to the eigenstate <k> of different electronic states belonging to the same monomer (base), *e.g.* the S_1 and S_2 states of each adenine or the S_1 state of thymine.

Figure 2A shows the participation ratio of the eigenstates obtained for one conformation and a single distribution of monomer excitation energy values. The PR values are quite spread, ranging from 1 (localization on a single base) to 3.6. The PR pattern becomes smoother when average

values over 500 distributions of diagonal terms are considered (Figure 2B). In the latter case, the values of participation ratio are comprised between 1.2 and 2.2. The eigenstates located at the edges of the exciton band have lower *PR* values.

Figure 3

The spatial extent of a given eigenstate can be illustrated by its energetic topography which is obtained by plotting the $(C_{k,m}^i)^2$ values as a function of the location of each base *m* within the double helix. Figure 3 shows the topography of four eigenstates having different participation ratios: 1.0, 1.6, 2.2 and 3.6. They concern the eigenstates $\langle 1 \rangle$, $\langle 10 \rangle$, $\langle 20 \rangle$ and $\langle 24 \rangle$ corresponding to the data in Figures 1a and 2a. We observe that each eigenstate exhibits a specific pattern. In the case of $\langle 1 \rangle$, 98% of the excitation is born by the S_1 state of the thymine N° 10. At this point it is important to notice that, in spite of the practically complete localization of $\langle 1 \rangle$ on a thymine chromophore, the associated oscillator strength (0.16) is lower than that of the thymine monomer (0.24). In other terms, the existence of delocalized states in the double helix perturbs also the properties of those which remain localized. The eigenstate $\langle 10 \rangle$ is mainly built on the S_2 states of the adenines N° 5, 6 and 7; we also note a small participation (about 7%) of the S_1 state corresponding to the thymines N° 3 to 5. In the case of $\langle 20 \rangle$, 77% of the excitation is located on the S_1 state of the adenine N°4 and the neighboring adenines share about 10% each. Finally, three adenines and four thymines participate to eigenstate $\langle 24 \rangle$. From the topographies in Figure 3, it appears that the various eigenstates, corresponding to the examined energy distribution and

configuration, extend over different parts of the double helix. Thus, if internal conversion among the eigenstates (intrabande scattering) occurs more rapidly than any other relaxation process, it would result to energy transfer along the double helix ($\langle 24 \rangle \rightarrow \langle 1 \rangle$) as well as between the two strands ($\langle 24 \rangle \rightarrow \langle 20 \rangle$).

It is difficult to draw a clear limit between localized and delocalized eigenstates. We propose to consider, in an arbitrary way, that an eigenstate is localized if, among the thirty coefficients $(C_{k,m}^i)^2$, there is one whose value is higher than 0.9. In other terms, delocalization occurs if at least 10% of the excitation is shared with one or more other bases. Following this definition, 75% of the eigenstates, calculated for 500 distributions of diagonal energies, can be viewed as delocalized although their extent is limited over only very few bases. Moreover, half of the spatially delocalized eigenstates are also electronically delocalized, in the sense that they result from mixing of different monomer states, for example, mixing of the thymine S_1 with the adenine S_1 or the adenine S_2 . This happens because the absorption bands associated with the monomer transitions largely overlap.

After having examined the effect of monomer spectral width on the oscillator strength and the spatial extent of the eigenstates corresponding to a single conformation of the duplex, we compare the influence of the conformational changes. Figures 1B and 2B shows the f and PR values per eigenstate which are obtained for four different conformations. We observe that both properties exhibit only a weak dependence on the geometry adopted by the duplex, arising from the variation of the off-diagonal terms.^[20]

The spatial extent of the duplex excited states may increase by the simultaneous action of

coulombic interactions and interactions due to orbital overlap (in particular interchromophore charge transfer). The calculation of this type of interactions is very tedious and has not been achieved so far for DNA double helices. Quantum chemistry calculations performed for stacked aromatic molecules have shown that orbital overlap interactions may be of the order of one hundred of wavenumbers.^[14-27] A very rough estimation of the combined action of dipolar coupling and orbital overlap interactions, can be made by adding a constant term of 100 cm^{-1} to the off-diagonal terms corresponding to nearest neighbors. For a base n , we considered as nearest neighbors the bases $n-1$ and $n+1$ on the same strand, and the bases $20-n$, $21-n$ and $22-n$ on the opposite strand. Figure 4 shows that, as expected, this additional coupling term makes the participation ratio twice as large.

Figure 4

The absorption spectrum corresponding to a given conformation of the duplex is constructed by plotting the oscillator strength of the thirty eigenstates obtained for each one of the 500 sets of monomer transition energy values. Figure 5 shows the spectrum calculated for a single conformation as well as the average obtained for four different conformations. A nanometer scale is used in the plots in order to make the connection with usual experimental conditions. We observe that, in line with what was found for the oscillator strength and the participation ratio, structural changes have only a weak influence on the spectrum profile.

Figure 5

The simulated duplex spectra, although similar to the experimental spectra, do not intend to strictly reproduce them. As a matter of fact, symmetric Gaussian curves were used to simulate the monomer transition energy, whereas the experimental bands are rather asymmetric. Moreover, at short wavelengths, higher order transitions overlap with those taken into account in the simulations. Finally, charge transfer interactions neglected here, are expected to induce a bathochromic shift of the duplex spectrum, as well as a change in the oscillator strength.^[15] In spite of the above limitations, the calculated spectra of $(dA)_{10} \cdot (dT)_{10}$ allows us to evidence the effect of the formation of delocalized excited states due to dipolar coupling. To this end, we compare them with the spectrum corresponding to non-interacting monomers, obtained by adding the three Gaussian curves which represent the energy distribution of three monomer transitions, the area under each Gaussian being proportional to the associated oscillator strength. We observe that the duplex spectra are only slightly shifted (7 nm at the maximum) to the blue with respect to the spectra of non-interacting monomers and, most importantly, they do not exhibit any apparent splitting.

It is interesting to visualize on the duplex absorption spectrum the position of the thirty eigenstates $\langle k \rangle$ and their participation ratios. This is shown in Figure 6 where data obtained for a single duplex conformation using 500 sets of the monomer energy distribution, that is, a total of 15000 values, are plotted. Each excited state $\langle k \rangle$ is represented by a linear segment (Figure 6A). We observe that the positions of the various eigenstates largely overlap. Regarding the dispersion of

the participation ratio over the absorption spectrum, we notice that the more extended eigenstates are located close to the absorption maximum (Figure 6B). In contrast, the eigenstates located near the spectral edges are rather localized on single bases. The plots in Figure 6 show that excitation at a given wavelength will populate eigenstates with different indexes, corresponding to various distributions of monomer energy transitions; their relative proportion depends on the associated oscillator strength. For example, laser excitation at 267 nm, already used for the study of such type of duplexes by femtosecond fluorescence spectroscopy,^[22] populates mainly eigenstates comprised between $\langle 10 \rangle$ and $\langle 20 \rangle$, which are the most delocalized and result from mixing of different monomer states. In contrast, laser excitation at 295 nm, used to study these compounds by single photon counting,^[5] creates mainly localized excited states.

Figure 6

SUMMARY AND COMMENTS

The main results of our theoretical study performed for the model duplex $(dA)_{10} \cdot (dT)_{10}$ can be summarized as follows.

1. The spectral width reduces the spatial extent of the duplex singlet excited states and increases the mixing between different types of monomer excited states (S_1 and S_2 of adenine, S_1 of thymine).
2. Most of the duplex excited states, calculated by taking into account only dipolar coupling, are delocalized over at least two bases. The degree of delocalization increases by the

combined action of coulombic and short range interactions. Short range interactions associated to interchromophore charge transfer, which have not been precisely calculated so far for double helices, could also be responsible for the well-known DNA hypochromism.

3. The properties of the duplex exciton states, whose calculation is based only on dipolar coupling, are not very sensitive to conformational changes.
4. The only difference between the duplex absorption spectra and those of non-interacting monomers is that the former are only slightly shifted to higher energies. This contrasts with what is commonly accepted, *e.g.* that delocalization of the excitation should induce large spectral shifts and an apparent splitting of the absorption band.
5. Excitation at various parts of the absorption spectrum leads to the formation of excited states with different degree of delocalization: small at the spectral edges, larger near the maximum.

Delocalization of the excitation over pairs of adjacent aminopurines, incorporated in a double stranded oligonucleotide, has been evidenced recently by fluorescence measurements.^[28]

Delocalization of the excitation over native bases, even if it is restricted to a short range, is expected to affect both energy transfer and excited state reactivity. The former, was implicitly considered to proceed via a hopping mechanism^[29-34] and, thus, limited by the extremely short fluorescence lifetimes of nucleic acids.^[21-35] Regarding the latter, one could wonder if, for example, cyclobutane dimer formation is favored or hindered when the energy of one photon is shared by two neighboring thymines. This type of questions may inspire experimental studies

aiming at the understanding of DNA photodamage within a novel context.

Acknowledgment. Financial support from the ACI “Physicochimie de la Matière Complexe” is gratefully acknowledged. We thank Dr B. Bouvier for helpful discussions and Dr J. P. Dognon for having provided us with the necessary infrastructure within his group.

FIGURE CAPTIONS

Figure 1. Oscillator strength corresponding to the 30 eigenstates of the duplex $(dA)_{10}.(dT)_{10}$. **(A)**: single conformation and single distribution of monomer transition energies, both chosen randomly. **(B)**: average values over 500 distributions of monomer transition energies; black, grey, white and dark grey bars correspond to four different conformations extracted from molecular dynamics simulations.

Figure 2. Participation ratio corresponding to the 30 eigenstates of the duplex $(dA)_{10}.(dT)_{10}$. **(A)**: single conformation and single distribution of monomer transition energies, both chosen randomly. **(B)**: average values over 500 distributions of monomer transition energies; black, grey, white and dark grey bars correspond to four different conformations extracted from molecular dynamics simulations.

Figure 3. Topography of the eigenstates $\langle 1 \rangle$, $\langle 10 \rangle$, $\langle 20 \rangle$ and $\langle 24 \rangle$ obtained for the same conformation of $(dA)_{10}.(dT)_{10}$ and the same set of monomer energy values as those corresponding to Figure 1A. The coefficients $(C_{k,m}^i)$ represent the contribution of chromophore m in its i^{th} excited state to eigenstate $\langle k \rangle$. The upper and lower parts of each histogram refer to chromophores located on each of the two strands.

Figure 4. Participation ratio associated with 30 the eigenstates corresponding to one conformation of $(dA)_{10}.(dT)_{10}$; average values over 500 distributions of monomer transition energies. White bars: only dipolar coupling is taken into account. Black bars: a constant equal to 100 cm^{-1} is added to the dipolar coupling acting between the five nearest neighbors on either strand (*cf.* inset).

Figure 5. Absorption spectrum of a single $(dA)_{10}.(dT)_{10}$ conformation (black line) calculated for 500 distributions of monomer transition energies. In grey: average spectrum corresponding to four different conformations. The dashed line represents the sum of the Gaussians corresponding to non-interacting monomers.

Figure 6. Position of the eigenstates (linear segments) and their participation ration (circles) with respect to the absorption spectrum obtained for a single conformation of $(dA)_{10}.(dT)_{10}$ and 500 sets of monomer excitation energy.

Table 1. Properties of the Gaussian curves representing the monomer transitions used in the calculation of the duplex $(dA)_{10} \cdot (dT)_{10}$ eigenstates.

transition		area (<i>f</i>)	maximum (cm^{-1})	width ($\text{fwhm}/\text{cm}^{-1}$)
Adenine	$S_0 \rightarrow S_1$	0.05	36700	2200
	$S_0 \rightarrow S_2$	0.24	38800	3600
Thymine	$S_0 \rightarrow S_1$	0.24	37500	4200

REFERENCES

- [1] J. Cadet, P. Vigny, *Bioorganic Photochemistry*, John Wiley & Sons, New York, **1990**, 1-272,
- [2] N. Dumaz, H. J. Van Kranen, A. De Vries, R. J. W. Berg, P. W. Wester, C. F. Van Kreijl, A. Sarasin, L. Daya-Grosjean, F. R. De Gruijl, *Carcinogenesis* **1997**, *18*, 897-904.
- [3] J. Eisinger, R. G. Shulman, *Science* **1968**, *161*, 1311-1319.
- [4] W. Rhodes, *J. Am. Chem. Soc.* **1961**, *83*, 3609-3617.
- [5] S. Georghiou, T. D. Bradrick, A. Philippetis, J. Beechem, *Biophys. J.* **1996**, *70*, 1909-1922.
- [6] I. Tinoco Jr., *J. Am. Chem. Soc.* **1960**, *82*, 4785-4790.
- [7] T. Miyata, S. Yomosa, *J. Phys. Soc. Jpn.* **1969**, *27*, 727-735.
- [8] R. N. Barnett, C. L. Cleveland, A. Joy, U. Landman, G. B. Schuster, *Science* **2001**, 567-571.
- [9] J. P. Lewis, T. E. Cheatham, III, E. B. Starikov, H. Wang, O. F. Sankey, *J. Phys. Chem. B* **2003**, *107*, 2581-2587.
- [10] S. Tanaka, Y. Sengoku, *Phys. Rev. E* **2003**, 68.
- [11] J. Frenkel, *Phys. Rev.* **1931**, *37*, 1276.
- [12] A. S. Davydov, *Theory of Molecular Excitons*, Plenum Press, New York, **1971**,
- [13] C. Ecoffet, D. Markovitsi, P. Millié, J. P. Lemaistre, *Chem. Phys.* **1993**, *177*, 629-643.

- [14] G. D. Scholes, K. P. Ghiggino, *J. Phys. Chem.* **1994**, *98*, 4580-4590.
- [15] G. D. Scholes, *J. Phys. Chem.* **1996**, *100*, 18731-18739.
- [16] X. Hu, T. Ritz, A. Damjanovic, K. Schulten, *J. Phys. Chem. B* **1997**, *101*, 3854-3871.
- [17] S. Marguet, D. Markovitsi, P. Millié, H. Sigal, S. Kumar, *J. Phys. Chem. B* **1998**, *102*, 4697-4710.
- [18] X. J. Jordanides, G. D. Scholes, G. R. Fleming, *J. Phys. Chem. B* **2001**, *105*, 1652-1669.
- [19] B. Bouvier, T. Gustavsson, D. Markovitsi, P. Millié, *Chem. Phys.* **2002**, *275*, 75-92.
- [20] B. Bouvier, J. P. Dognon, R. Lavery, D. Markovitsi, P. Millié, D. Onidas, K. Zakrzewska, *J. Phys. Chem. B* **2003**, *107*, 13512-13522.
- [21] D. Onidas, D. Markovitsi, S. Marguet, A. Sharonov, T. Gustavsson, *J. Phys. Chem. B* **2002**, *106*, 11367- 11374.
- [22] D. Markovitsi, D. Onidas, A. Sharonov, T. Gustavsson, *ChemPhysChem* **2003**, *3*, 303-305.
- [23] T. Förster, **1965**, 93-137.
- [24] D. Markovitsi, L. K. Gallos, J. P. Lemaistre, P. Argyrakis, *Chem. Phys.* **2001**, *269*, 147-158.
- [25] P. Dean, *Rev. Mod. Phys.* **1972**, *44*, 127-169.
- [26] M. Schreiber, Y. Toyosawa, *J. Phys. Soc. Jpn.* **1982**, *51*, 1537-1543.
- [27] G. D. Scholes, I. R. Gould, R. J. Cogdell, G. R. Fleming, *J. Phys. Chem. B* **1999**, *103*, 2543-2553.

- [28] M. Rist, H.-A. Wagenknecht, T. Fiebig, *ChemPhysChem* **2002**, *8*, 704-707.
- [29] M. Guéron, J. Eisinger, R. G. Shulman, *J. Chem. Phys.* **1967**, *47*, 4077- 4091.
- [30] D. M. Rayner, A. G. Szabo, R. O. Loutfy, R. W. Yip, *J. Phys. Chem.* **1980**, *84*, 289-293.
- [31] S. Georghiou, S. Zhu, R. Weidner, C.-R. Huang, G. Ge, *J. Biomol. Struct.* **1990**, *8*, 657- 674.
- [32] G. Ge, S. Georghiou, *Photochem. Photobiol.* **1991**, *54*, 301- 305.
- [33] S. Georghiou, G. R. Phillips, G. Ge, *Biopolymers* **1992**, *32*, 1417- 1420.
- [34] C.-R. Huang, S. Georghiou, *Photochem. Photobiol.* **1992**, *56*, 95- 99.
- [35] J. Peon, A. H. Zewail, *Chem. Phys. Lett.* **2001**, *348*, 255-262.

Table of contents text

The simulated absorption spectra of the model DNA duplex $(dA)_{10} \cdot (dT)_{10}$ are very similar to those of non-interacting monomers. Most of the excited states are delocalized over at least two bases and result from mixing of different monomer states. The states with larger spatial extent are located close to the maximum of the absorption spectrum.

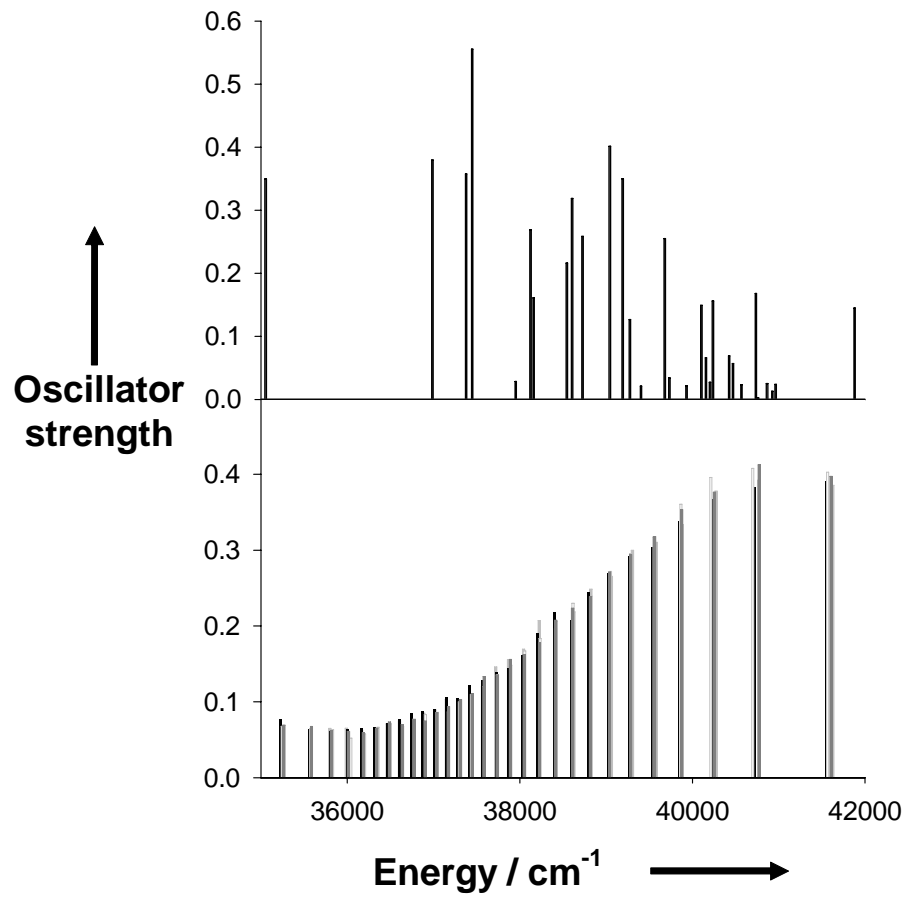
Figure 1

Figure 2

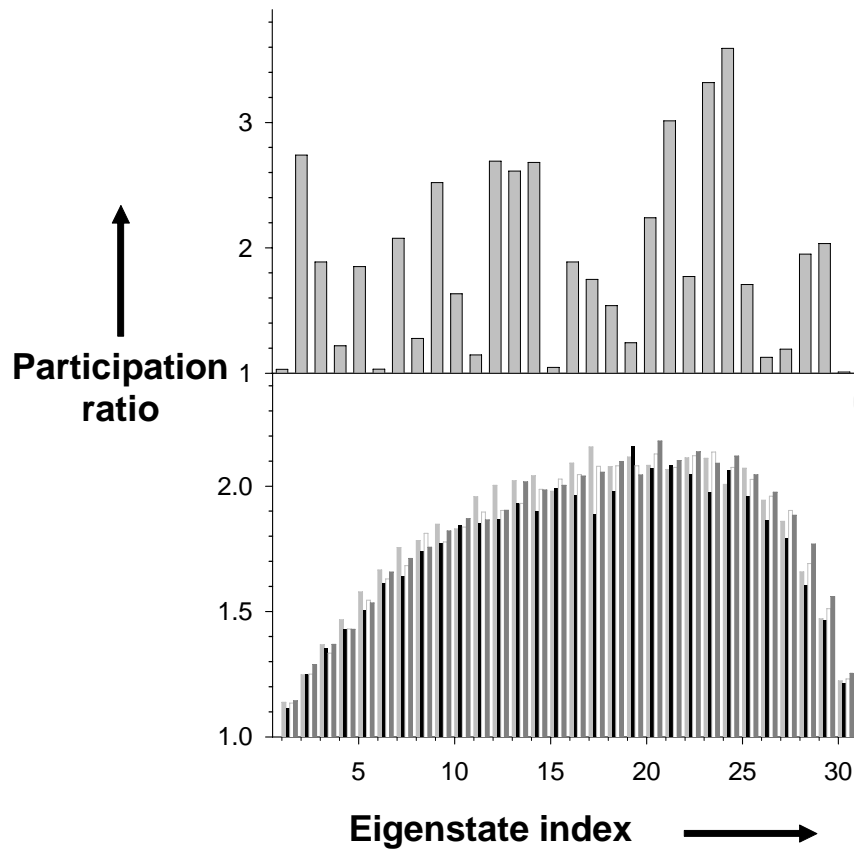


Figure 3

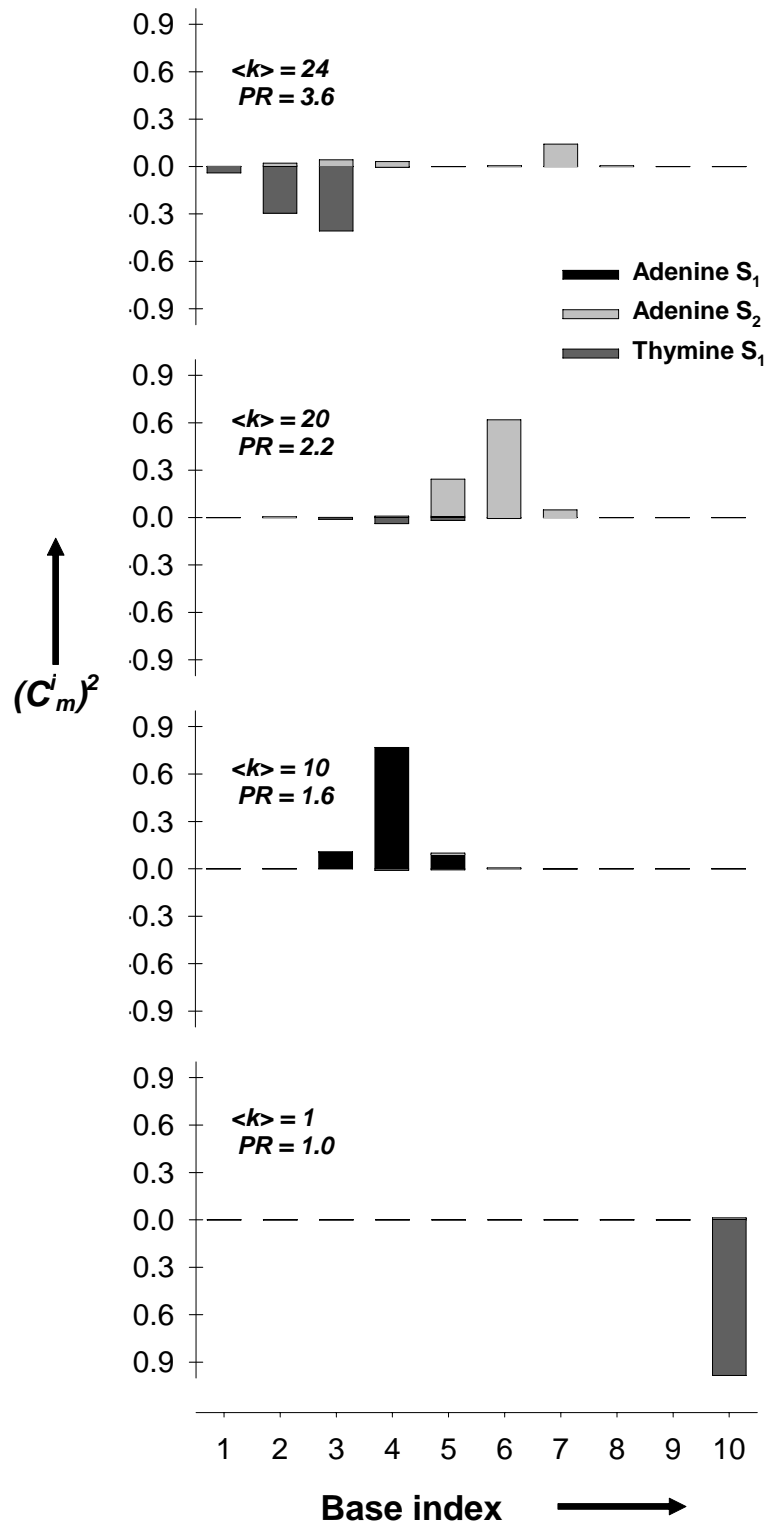


Figure 4

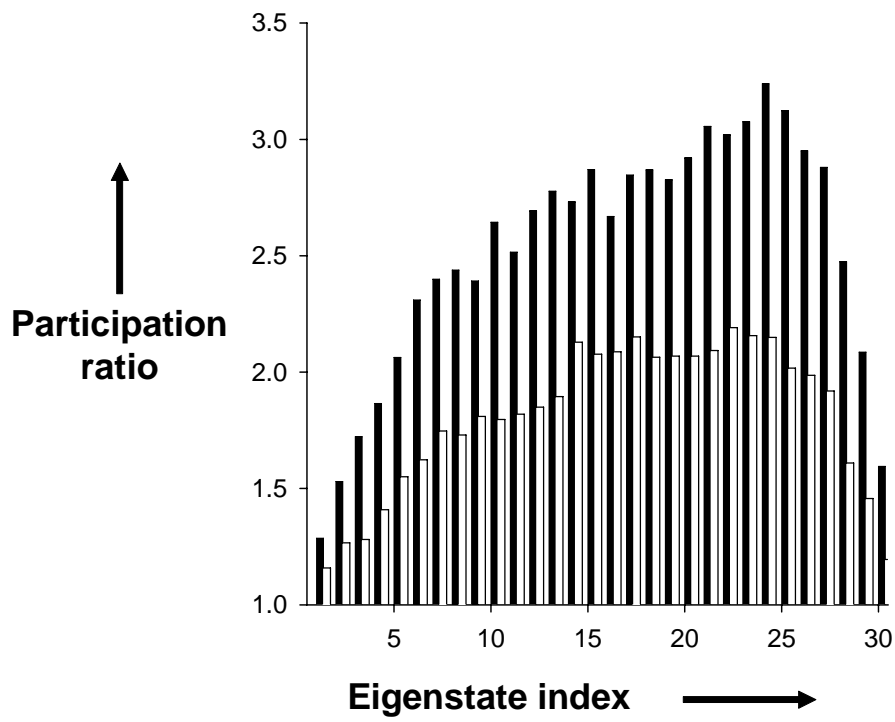


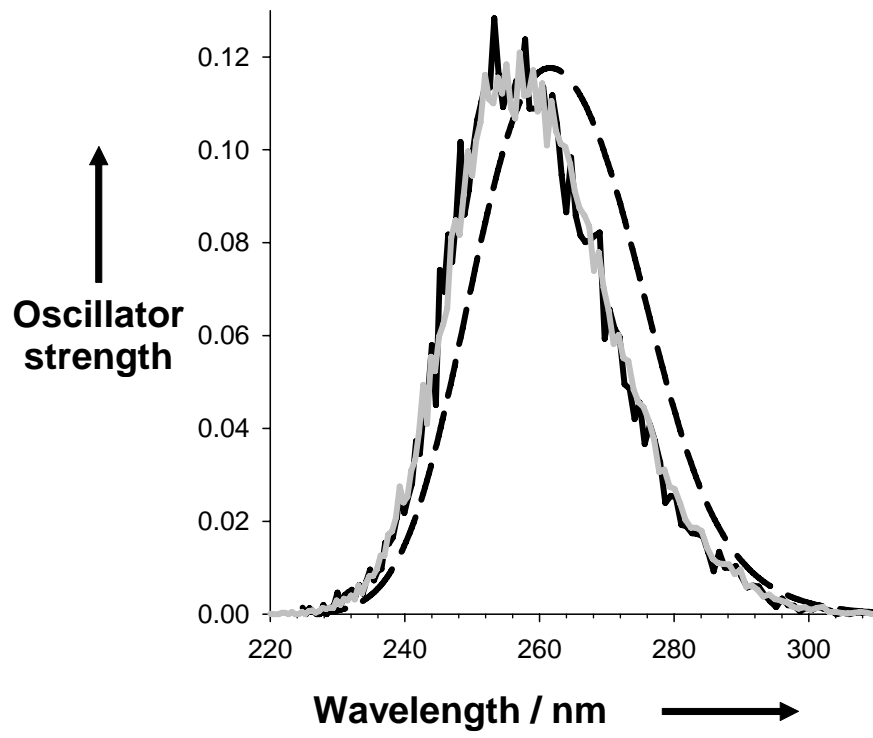
Figure 5

Figure 6

